Technical note

HAMAMATSU
PHOTON IS OUR BUSINESS

Compound opto-semiconductor photosensors

Contents

Compound semiconductor photosensors are opto-semiconductors made of two or more elements mainly from groups II to VI. These photosensors have different spectral response ranges depending on the elements comprising them. This means photosensors can be made that are sensitive to different wavelengths from the ultraviolet to infrared region. Hamamatsu provides detectors for many different wavelengths by taking advantage of its expertise in compound semiconductor technology accumulated over many years. We offer an especially wide detector product lineup in the infrared region. Applications for our compound semiconductor photosensors range from academic research to information communication devices and general-purpose electronic equipment.

Spectral response of compound semiconductor photosensors (typical example)

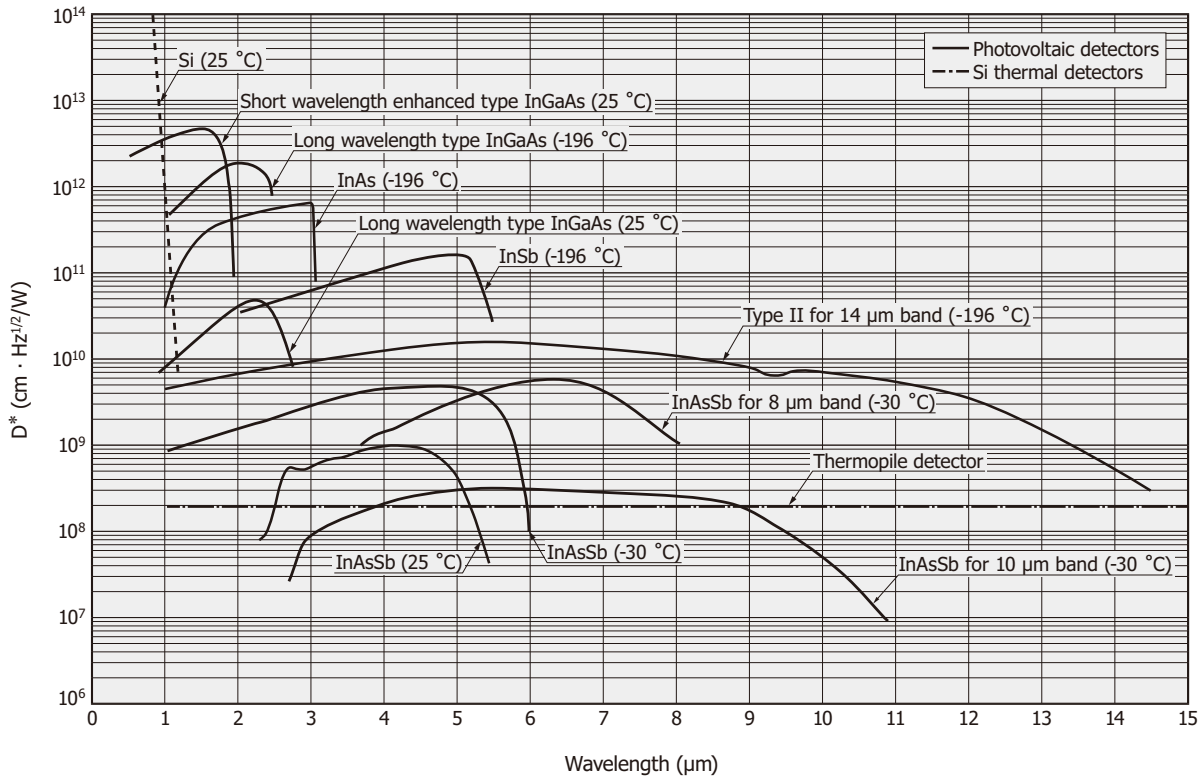

KIRDB0259ES

Hamamatsu compound semiconductor photosensors

Product name	Spectral response range (μm)	Features
InGaAs PIN photodiodes	0.5 – 1.7	● Short-wavelength enhanced type ● Can detect light from 0.5 μm
	0.9 – 1.7	● Standard type ● High-speed response, high sensitivity, low dark current ● Various types of photosensitive areas, arrays, and packages available
	0.9 – 1.9	● For light measurement around 1.7 μm ● TE-cooled type available
	0.9 – 2.1	● For light measurement in water absorption band (1.9 μm) ● TE-cooled type available
	0.9 – 2.6	● For NIR spectrometry ● TE-cooled type available
InGaAs APD	0.95 – 1.7	● High sensitivity, high-speed response, low capacitance, low dark current ● Various sizes of photosensitive areas available

Product name		Spectral response range (μm)	Features
InAs photovoltaic detectors		1 – 3.8	● Covers a spectral response range close to PbS but offers higher response speed
InSb photovoltaic detectors		1 – 5.5	● High sensitivity in so-called atmospheric window (3 to 5 μm) ● High-speed response
InAsSb photovoltaic detectors		1 – 11	● Infrared detector with cutoff wavelength of 5 μm, 8μm or 10 μm bands ● High-speed response and high reliability
Type Ⅱ superlattice infrared detector		1 – 14.5	● InAs and GaSb superlattice structure enables the detection up to around 14.5 μm
Two-color detectors	Si + InGaAs	0.32 – 2.55	● Wide spectral response range ● Incorporates two photosensors with different spectral response ranges on top of each other on the same optical axis
	Si + InAsSb	0.32 – 5.3	
	Standard type InGaAs + long wavelength type InGaAs	0.9 – 2.55	

1. InGaAs PIN photodiodes

InGaAs PIN photodiodes are photovoltaic detectors having PN junction just the same as Si photodiodes.

[Figure 1-1] Spectral response

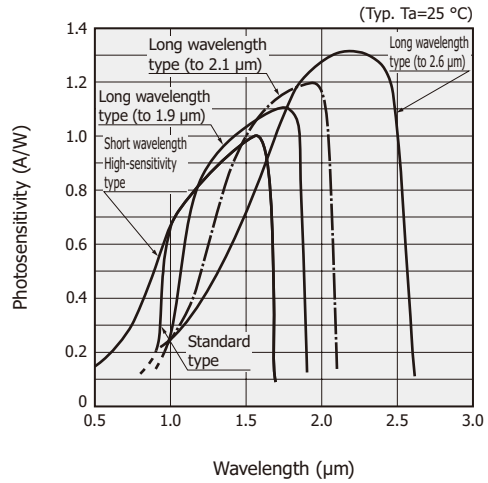

KIRDB0332EF

InGaAs has a smaller band gap energy compared to Si, so it is sensitive to longer wavelengths. Since the InGaAs band gap energy varies depending on the composition ratio of In and Ga [Figure 1-2], infrared detectors with different spectral response ranges can be fabricated by just changing this composition ratio. Hamamatsu provides standard types having a cutoff wavelength of 1.7 µm, short-wavelength enhanced types, and long wavelength types having a cutoff wavelength extending to 1.9 µm or 2.1 µm or up to 2.6 µm.

[Figure 1-2] Band gap energy vs. composition ratio x of InxGa1-xAs

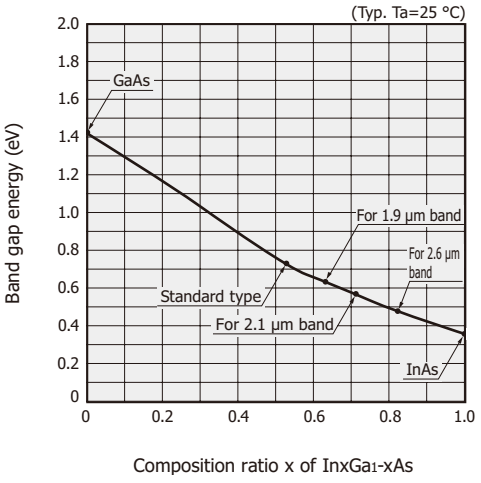

KIRDB0130EB

1 - 1 Characteristics

» Current vs. voltage characteristics

When voltage is applied to an InGaAs PIN photodiode in a dark state, current vs. voltage characteristics like that shown in Figure 1-3 (a) are obtained. When light enters the photodiode, this curve shifts as shown at ② in Figure 1-3 (b). As the light level is increased, the curve further shifts as shown at ③. Here, when both terminals of the photodiode are left open, an open circuit voltage (Voc) appears in the forward direction. When both terminals are shorted, a short circuit current (Isc) flows in the reverse direction.

Figure 1-4 shows methods for measuring the light level by detecting the photocurrent. In Figure 1-4 (a), a load resistor is connected and the voltage Io × RL is amplified by an amplifier having a gain of G. In this circuit, the linearity range is limited [Figure 1-3 (c)].

Figure 1-4 (b) shows a circuit connected to an op amp. If we set the open-loop gain of the op amp as A, then the equivalent input resistance becomes Rf/A due to negative feedback circuit characteristics. This resistance is several orders of magnitude smaller than the input resistance of the circuit in Figure 1-4 (a), allowing ideal measurement of the short circuit current (Isc). If the short circuit current must be measured over a wide range, then change the Rf as needed.

[Figure 1-3] Current vs. voltage characteristics

(a) In dark state

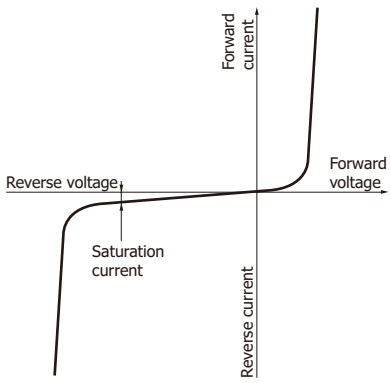

KIRDC0030EA

(b) When light is incident

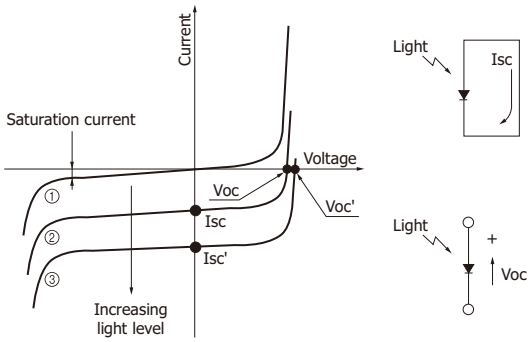

KPDC0005EA

(c) Current vs. voltage characteristics and load line

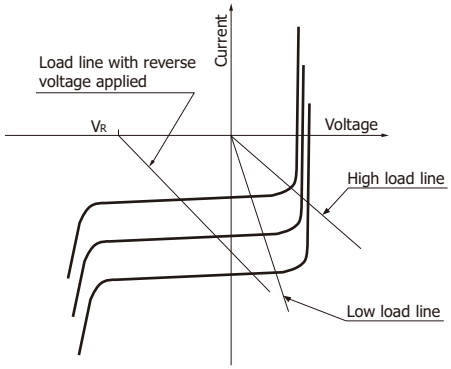

KPDB0003EB

[Figure 1-4] Connection examples

(a) When load resistor is connected

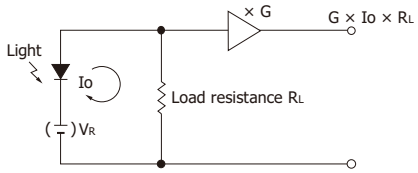

(b) When op amp is connected

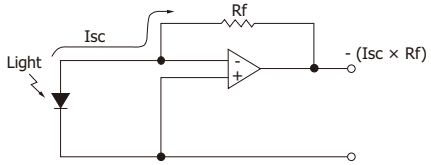

KPDC0006ED

Equivalent circuit

A circuit equivalent to an InGaAs PIN photodiode is shown in Figure 1-5. The short circuit current (Isc) is expressed by equation (1-1). The linearity limit of the short circuit current is determined by the 2nd and 3rd terms of this equation.

$$Isc = I_L - Is\left[\exp\frac{q\,(Isc \times Rs)}{k\,T} - 1\right] - \frac{Isc \times Rs}{Rsh} \quad \cdots\cdots\cdots (1\text{-}1)$$

I_L : current generated by incident light (proportional to light level)
Is : photodiode reverse saturation current
q : electron charge
Rs : series resistance
k : Boltzmann's constant
T : absolute temperature of photodiode
Rsh: shunt resistance

[Figure 1-5] Equivalent circuit

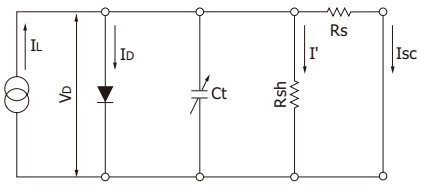

KPDC0004EB

V_D: voltage across diode
I_D : diode current
Ct : terminal capacitance
I' : shunt resistance current
Vo: output voltage
Io : output current

Linearity

The lower limit of InGaAs PIN photodiode linearity is determined by noise while the upper limit is determined by the chip structure and composition, photosensitive area size, electrode structure, incident light spot size, and the like. To expand the upper limit, a reverse voltage is applied in some cases. However, applying 1 V is sufficient if only the linearity needs to be considered. Figure 1-7 shows connection examples for applying a reverse voltage. Although applying a reverse voltage is useful to improve the linearity or response characteristics, it also results in larger dark current and higher noise level. Excessive reverse voltages might also damage or deteriorate the photodiode, so always use the reverse voltage that is within the absolute maximum rating and set the polarity so that the cathode is at positive potential relative to the anode.

[Figure 1-6] Linearity

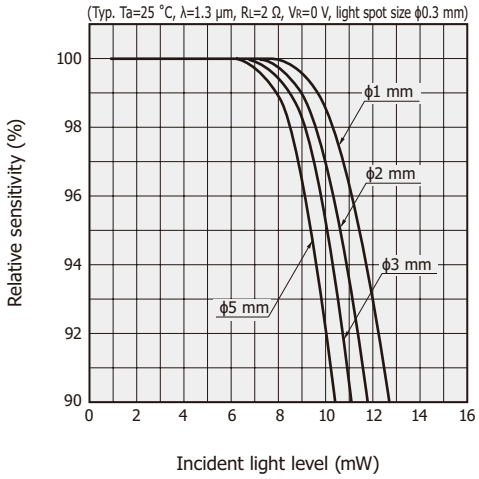

KIRDB0333EB

[Figure 1-7] Connection examples (with reverse voltage applied)

(a) When load resistor is connected

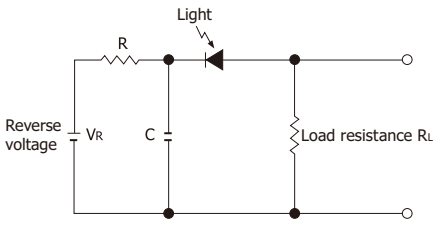

(b) When op amp is connected

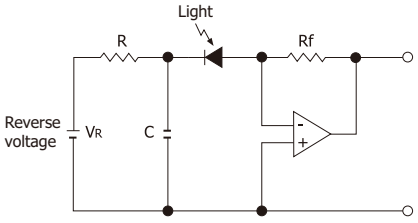

KPDC0008EB

Noise characteristics

Like other typical photosensors, the lower limits of light detection for InGaAs PIN photodiodes are determined by their noise characteristics. Noise current (in) in a photodiode is the sum of the thermal noise current (or Johnson noise current) ij of a resistor, which approximates the shunt resistance Rsh, and the shot noise currents i_{SD} and i_{SL} resulting from the dark current and the photocurrent, respectively [equation (1-2)].

$$in = \sqrt{ij^2 + i_{SD}^2 + i_{SL}^2} \ [A] \quad \cdots\cdots\cdots (1\text{-}2)$$

If a reverse voltage is not applied as in Figure 1-4, then ij is given by equation (1-3).

$$ij = \sqrt{\frac{4k\,T\,B}{Rsh}} \ [A] \quad \cdots\cdots\cdots (1\text{-}3)$$

k: Boltzmann's constant
T: absolute temperature of element
B: noise bandwidth

When a reverse voltage is applied as in Figure 1-7, then there is always a dark current and the i_{SD} is as shown in equation (1-4).

$$i_{SD} = \sqrt{2q\,I_D\,B} \ [A] \quad \cdots\cdots\cdots (1\text{-}4)$$

q : electron charge
I_D: dark current

If photocurrent (I_L) is generated by incident light and $I_L >> 0.026/Rsh$ or $I_L >> I_D$, then the shot noise current resulting from the photocurrent is a predominant source of noise current expressed by equation (1-5).

$$in \simeq i_{SL} = \sqrt{2q\,I_L\,B} \ [A] \quad \cdots\cdots\cdots (1\text{-}5)$$

The amplitude of these noise sources are each proportional to the square root of noise bandwidth (B) and so are expressed in units of $A/Hz^{1/2}$ normalized by B. The lower limit of light detection for photodiodes is usually expressed as the incident light level required to generate a current equal to the noise current as expressed in equation (1-3) or (1-4), which is termed the noise equivalent power (NEP).

$$NEP = \frac{in}{S} \ [W/Hz^{1/2}] \quad \cdots\cdots\cdots (1\text{-}6)$$

in: noise current
S : photosensitivity

In the circuit shown in Figure 1-7 (b), noise from the op amp and Rf must be taken into account along with the photodiode noise described above. Moreover, in high-frequency regions the transfer function including capacitive components such as photodiode capacitance (Ct) and feedback capacitance (Cf) must also be considered. The lower limit of light detection will be larger than the NEP defined in equation (1-6) because there are effects from the amplifier's temperature drift and flicker noise in low-frequency regions, gain peaking described later on, and others.
In the case of InGaAs PIN photodiodes, cooled types are often used to improve the lower limit of light detection. Periodically turning the incident light on and off by some means and synchronously detecting only signals of the same frequency are also effective in removing noise from unwanted bands. This allows the detection limit to approach the NEP [Figure 1-8].

[Figure 1-8] Synchronous detection method

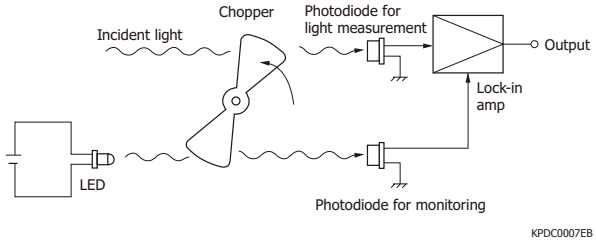

Spectral response

InGaAs PIN photodiodes are roughly divided into the following three types according to their spectral response ranges.

① Standard type:
sensitive in a spectral range from 0.9 to 1.7 µm
② Short-wavelength enhanced type:
variant of the standard type and having increased sensitivity to shorter wavelengths
③ Long wavelength type:
sensitive in a spectral range extending to longer wavelengths than standard type

The cutoff wavelength (λc) on the long wavelength side of photodiodes is expressed by equation (1-7) using their band gap energy (Eg).

$$\lambda c = \frac{1.24}{Eg} \ [\mu m] \quad \cdots\cdots\cdots (1\text{-}7)$$

Eg: band gap energy [eV]

The InGaAs light absorption layer in the standard type and short-wavelength enhanced type has a band gap energy of 0.73 eV. In the long wavelength type, this band gap energy is reduced by changing the ratio of elements making up the InGaAs light absorption layer in order to extend the cutoff wavelength to the longer wavelength side.
InGaAs PIN photodiodes are fabricated with a semiconductor layer called the cap layer which is formed on the InGaAs light absorption layer to suppress the surface leakage current that can cause noise. Light at wavelengths shorter than the cutoff wavelength of the

semiconductor comprising the cap layer is almost totally absorbed by the cap layer and so does not reach the light absorption layer, and therefore does not contribute to sensitivity. In the short-wavelength enhanced type, this cap layer is thinned to less than 1/10th the cap layer thickness for the standard type by improving the wafer structure and wafer process. This reduces the amount of light absorbed by the cap layer and so increases the amount of light reaching the light absorption layer, improving the sensitivity at short wavelengths.

Because the band gap energy increases as the chip temperature is lowered, the spectral response range of InGaAs PIN photodiodes shifts to the shorter wavelength side as the chip temperature decreases. This also reduces the amount of noise, so D* (detectivity) increases [Figure 1-10]. The spectral transmittance of the window materials used in the InGaAs/GaAs PIN photodiodes is shown in Figure 1-11.

[Figure 1-9] Spectral response

(a) Standard type

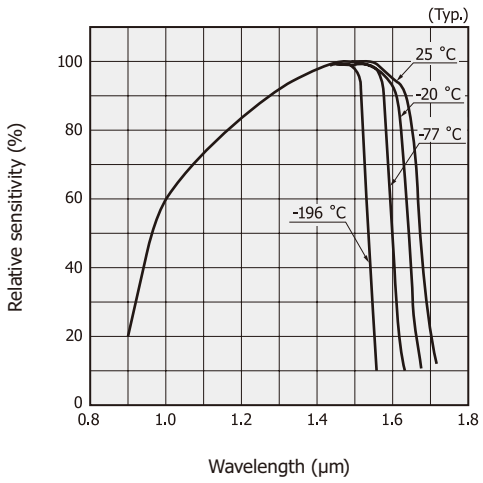

(b) Short-wavelength enhanced type

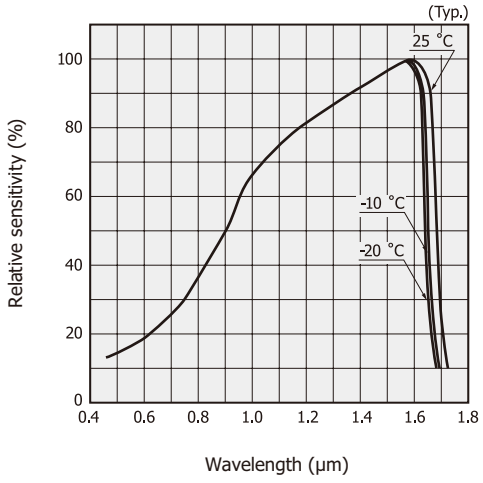

(c) Long wavelength type (up to 2.6 µm)

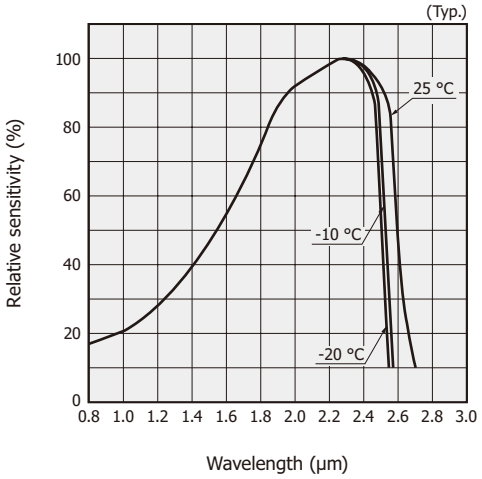

[Figure 1-10] D* vs. wavelength

(a) Standard type

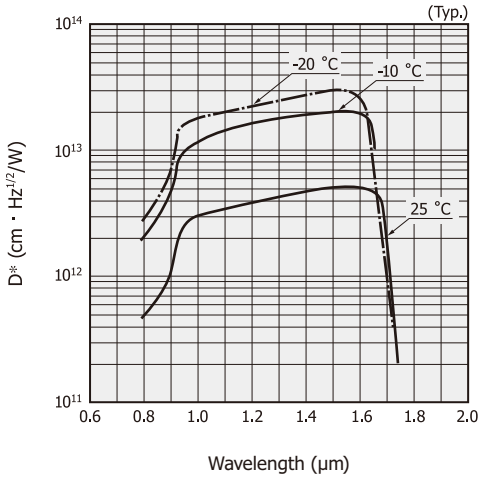

(b) Long wavelength type (up to 2.6 µm)

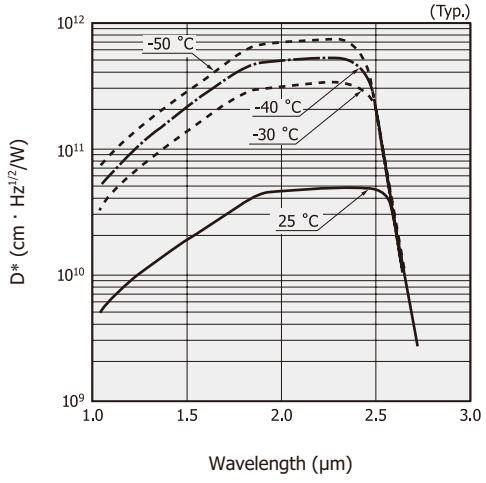

[Figure 1-11] Spectral transmittance of window materials (typical example)

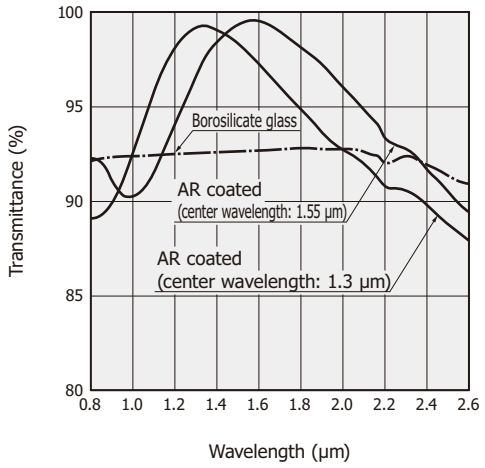

KIRDB0550EA

Response speed

The response speed is a measure of how fast the generated carriers are extracted to an external circuit as output current, and is generally expressed as the rise time or cutoff frequency.

The rise time (tr) is the time required for the output signal to rise from 10% to 90% of its peak value and is expressed by equation (1-8).

$$tr = 2.2Ct\ (R_L + Rs) \quad \cdots\cdots\cdots (1\text{-}8)$$

Ct: terminal capacitance
RL: load resistance
Rs: series resistance

Generally, Rs can be disregarded because $R_L >> Rs$. To make the rise time smaller, the Ct and RL should be lowered, but RL is determined by an external factor and so cannot freely be changed. Ct is proportional to the photosensitive area (A) and is inversely proportional to the square root of the reverse voltage (V_R).

$$Ct \propto \frac{A}{\sqrt{V_R}} \quad \cdots\cdots\cdots (1\text{-}9)$$

Higher response speeds can be obtained by applying a reverse voltage to a photodiode with a small photosensitive area.

Charges generated by light absorbed outside the PN junction sometimes take several microseconds or more to diffuse and reach the electrode. When the time constant of Ct × RL is small, this diffusion time determines response speeds. In applications requiring fast response, be careful not to allow light to strike outside the photosensitive area.

The approximate relationship between the rise time tr (unit: s) and cutoff frequency fc (unit: Hz) is expressed by equation (1-10).

$$tr = \frac{0.35}{fc} \quad \cdots\cdots\cdots (1\text{-}10)$$

For details on response speed, see “Si photodiodes technical note | 2. Characteristics | 2-6 Response speed.”

[Figure 1-12] Terminal capacitance vs. reverse voltage (standard type)

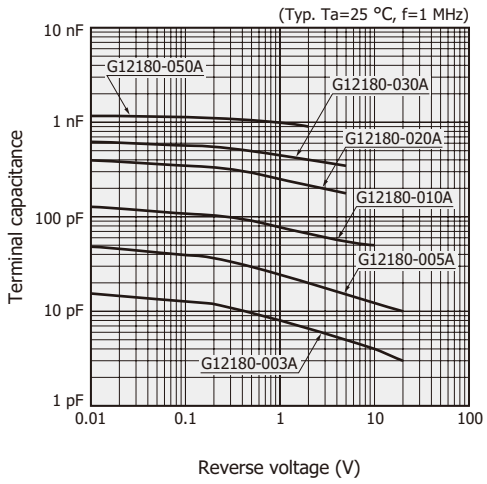

KIRDB0678EA

Figure 1-13 shows a high-speed light detection circuit using an InGaAs PIN photodiode. This is a specific example of a connection based on the circuit shown in Figure 1-7 (a) and uses a 50 Ω load resistance. The series resistance R and ceramic capacitor C reduce the noise from the reverse voltage power supply and also reduce the power supply impedance seen from the photodiode. The resistance R also functions to protect the photodiode, and its value should be selected so that the voltage drop caused by the maximum photocurrent will be sufficiently smaller than the reverse voltage. The photodiode and capacitor leads, coaxial cable wires, and the like carrying high-speed pulses should be kept as short as possible.

[Figure 1-13] High-speed light detection circuit

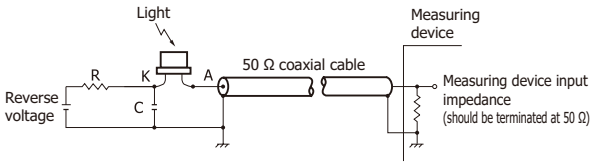

KPDC0009EA

Temperature characteristics

The spectral response and dark current change with the chip temperature. Figure 1-14 shows temperature characteristics of shunt resistance of InGaAs PIN photodiodes. Here, decreasing the chip temperature reduces the dark current and increases the shunt resistance and thereby improves the S/N.

The dark current increases exponentially as the

chip temperature rises. The relationship between the dark current IDx of the chip temperature x and the dark current IDy of the chip temperature y is given by equation (1-11). The dark current temperature coefficient "a" varies depending on the band gap energy of the detector. It also varies depending on the reverse voltage applied to the detector.

$$I_{Dx} = I_{Dy} \times a^{x-y} \cdots\cdots\cdots (1\text{-}11)$$

Hamamatsu provides one-stage and two-stage TE-cooled InGaAs PIN photodiodes that can be used at a constant operating temperature (or by cooling).

[Figure 1-14] Shunt resistance vs. chip temperature (standard type)

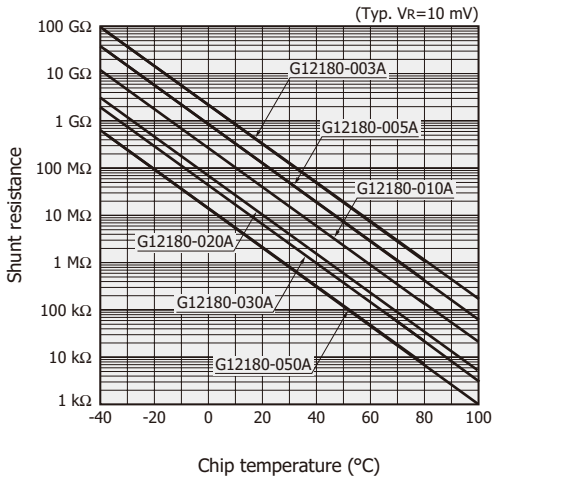

KIRDB0544EB

1 - 2 How to use

» Connection to an op amp

A connection example with an op amp is shown in Figure 1-15. The input impedance of the op amp circuit in Figure 1-15 is the value of the feedback resistance Rf divided by the open-loop gain and so is very small. This yields excellent linearity.

[Figure 1-15] Connection example

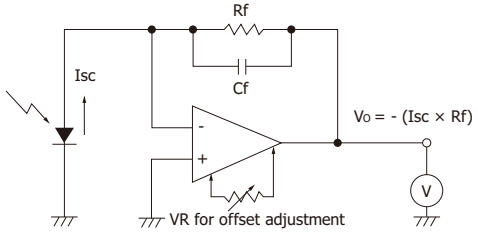

KIRDC0040EB

Precautions when using an op amp are described below.

(1) Selecting feedback resistance

In Figure 1-15, the short circuit current Isc is converted to the output voltage Vo, which is Isc × Rf. If Rf is larger than the photodiode shunt resistance Rsh, then the op amp's input noise voltage and input offset voltage are multiplied by (1 + Rf/Rsh) and superimposed on the output voltage. The op amp bias current error also increases, so there is a limit to the Rf increase.
The feedback capacitance Cf is mainly used to prevent oscillation. A capacitance of several picofarads is sufficient for this purpose. This feedback circuit has a time constant of Cf × Rf and serves as a noise filter. It also limits the response speed at the same time, so the feedback resistance value must be carefully selected to match the application. Error due to an offset voltage can usually be reduced to less than 1 mV by connecting a variable resistor to the offset adjustment terminals on the op amp. For application circuit examples, see "Si photodiodes technical note | 3. How to use | 3-2 Application circuit examples".

(2) Selecting an op amp

Since the actual input impedance of an op amp is not infinite, some bias current will flow into or out of the input terminals. This might cause an error in the output voltage value depending on the amplitude of the detected current.
The bias current which flows in an FET-input op amp is sometimes lower than 0.1 pA. Bipolar op amps, however, have bias currents ranging from several hundred picoamperes to several hundred nanoamperes.
In general, the bias current of FET-input op amps doubles for every 10 °C increase in temperature, while the bias current of bipolar op amps decreases. Because of this, bipolar type op amps also need to be considered when designing circuits for high temperature applications. Just as with offset voltages, the error voltage due to a bias current can be fine-tuned by connecting a variable resistor to the offset adjustment terminals of the op amp.

2. InGaAs APD

InGaAs APDs (avalanche photodiodes) are infrared detectors having an internal multiplication function. When an appropriate reverse voltage is applied, they multiply photocurrent to achieve high sensitivity and high-speed response.
InGaAs APDs are sensitive to light in the 1 µm band where optical fibers exhibit low loss, and so are widely used for optical fiber communications. Light in the 1 µm band is highly safe for human eyes (eye-safe) and is also utilized for FSO (free space optics) and optical distance measurement.

2 - 1 Operating principle

When electron-hole pairs are generated in the depletion layer of an APD with a reverse voltage applied to the PN junction, the electric field created across the PN junction causes the electrons to drift toward the N^+ side and the holes to drift toward the P^+ side. The drift speed of these carriers depends on the electric field strength. However, when the electric field is increased, the carriers are more likely to collide with the crystal lattice so that the drift speed becomes saturated at a certain speed. If the reverse voltage is increased even further, some carriers that escaped collision with the crystal lattice will have a great deal of energy. When these carriers collide with the crystal lattice, ionization takes place in which electron-hole pairs are newly generated. These electron-hole pairs then create additional electron-hole pairs in a process just like a chain reaction. This is a phenomenon known as avalanche multiplication. APDs are photodiodes having an internal multiplication function that utilizes this avalanche multiplication.

[Figure 2-1] Structure and electric field profile

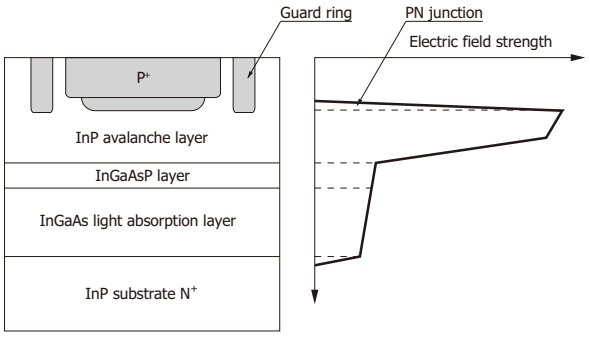

KIRDC0126EA

Because the band gap energy of InGaAs is small, applying a high reverse voltage increases the dark current. To cope with this, InGaAs APDs employ a structure in which the InGaAs light absorption layer that generates electron-hole pairs by absorbing light is isolated from the InP avalanche layer that multiplies carriers generated by light utilizing avalanche multiplication. APDs with this structure for separating the light absorption layer from the avalanche layer are called the SAM (separated absorption and multiplication) type. Hamamatsu InGaAs APDs employ this SAM type.

2 - 2 Characteristics

» Dark current vs. reverse voltage characteristics

APD dark current I_D consists of two dark current components: I_{DS} (surface leakage current and the like flowing through the interface between the PN junction and the surface passivation film) which is not multiplied, and I_{DG} (recombination current, tunnel current, and diffusion current generated inside the semiconductor, specified at M=1) which is multiplied.

$$I_D = I_{DS} + M \cdot I_{DG} \cdots\cdots (2\text{-}1)$$

Figure 2-2 shows an example of current vs. reverse voltage characteristics for an InGaAs APD. Since the InGaAs APD has the structure shown in Figure 2-1, there is no sensitivity unless the depletion layer extends to the InGaAs light absorption layer at a low reverse voltage.

[Figure 2-2] Dark current, and gain vs. reverse voltage (G14858-0020AA)

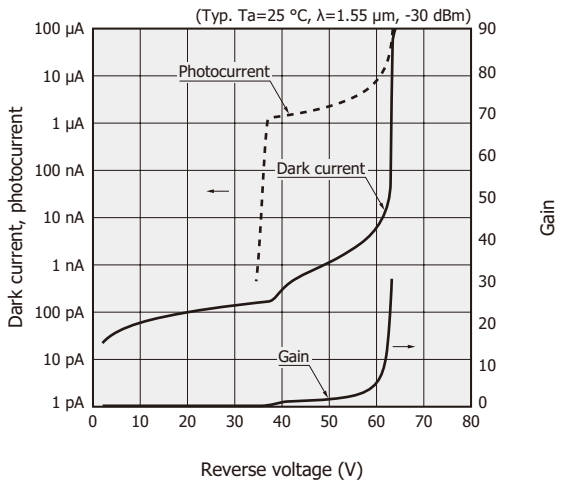

KAPDB0423EA

In our InGaAs APDs, under the condition that they are not irradiated with light, the reverse voltage that causes a reverse current of 100 µA to flow is defined as the breakdown voltage (V_{BR}), and the reverse current at a reverse voltage $V_R = 0.9 \times V_{BR}$ is defined as the dark current.

Gain vs. reverse voltage characteristics

InGaAs APD gain characteristics depend on the electric field strength applied to the InP avalanche layer, so the gain usually increases as the reverse voltage is increased. But increasing the reverse voltage also increases the dark current, and the electric field applied to the InP avalanche layer decreases due to a voltage drop in the series resistance component of the photodiode. This means that the gain will not increase even if the reverse voltage is increased higher than that level. If the APD is operated at or near the maximum gain, the voltage drop in the serial resistance component will become large, causing a phenomenon in which photocurrent is not proportional to the incident light level.

[Figure 2-3] Temperature characteristics of gain (G14858-0020AA)

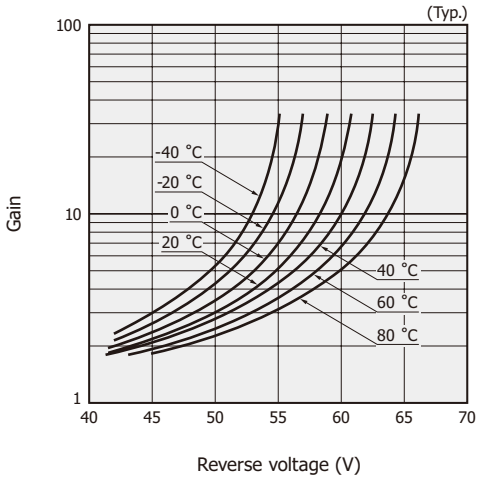

InGaAs APD gain varies with temperature as shown in Figure 2-3. The gain at a certain reverse voltage becomes smaller as the temperature rises. This phenomenon occurs because the crystal lattice vibrates more heavily as the temperature rises, increasing the possibility that the carriers accelerated by the electric field may collide with the lattice before reaching an energy level sufficient to cause ionization. To obtain a stable output, the reverse voltage must be adjusted to match changes in temperature or the chip temperature must be kept constant.
Figure 2-4 is a graph showing the temperature dependence of dark current vs. reverse voltage characteristics in the range from -40 to +80 °C.

[Figure 2-4] Temperature characteristics of dark current (G14858-0020AA)

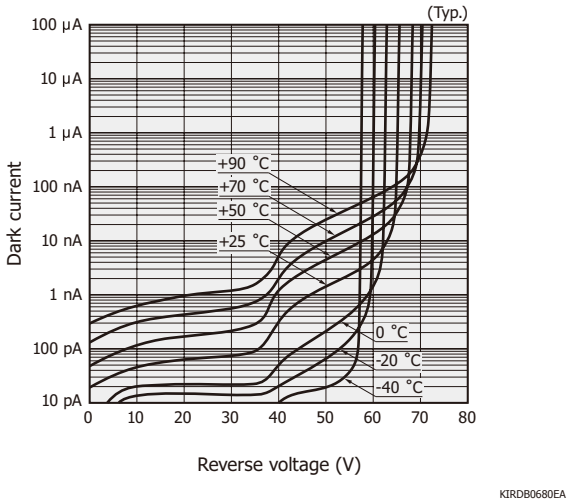

Temperature characteristic of breakdown voltage is shown in Figure 2-5.

[Figure 2-5] Breakdown voltage vs. temperature (G14858-0020AA)

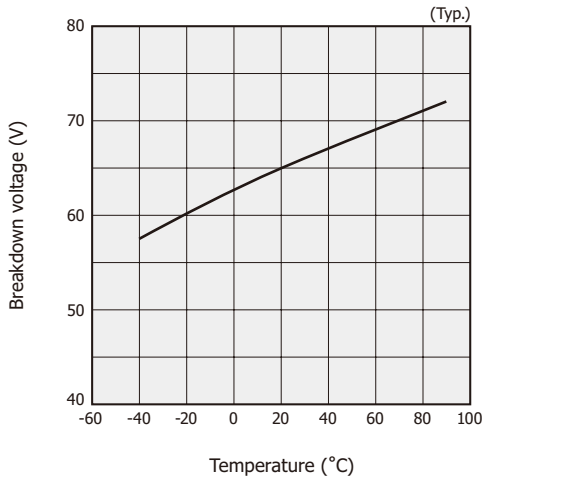

Spectral response

When light with energy higher than the band gap energy of the semiconductor is absorbed by the photodiode, electron-hole pairs are generated and detected as signals. The following relationship exists between the band gap energy Eg (unit: eV) and the cutoff wavelength λc (unit: µm), as shown in equation (2-2).

$$\lambda c = \frac{1.24}{Eg} \text{ [µm]} \quad \cdots\cdots \text{(2-2)}$$

As light absorption material, InGaAs APDs utilize InGaAs whose composition is lattice-matched to InP. The band gap energy of that material is 0.73 eV at room temperature. The InGaAs APD cutoff wavelength is therefore approx. 1.7 µm.

The InGaAs APD spectral response differs depending on the gain [Figure 2-6]. Sensitivity on the shorter wavelength side decreases because short-wavelength light is absorbed by the InP cap layer.

[Figure 2-6] Spectral response (G14858-0020AA)

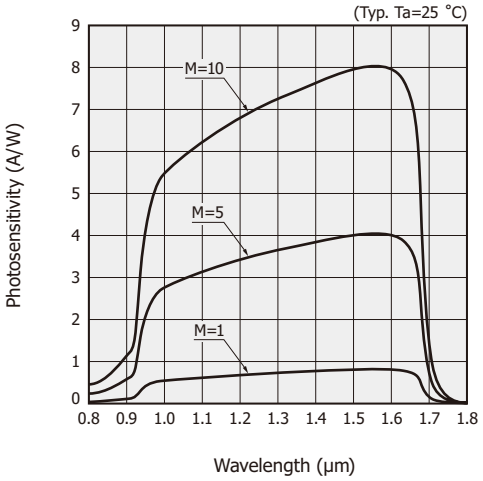

KIRDB0686EA

Temperature characteristics of the InGaAs band gap energy affect temperature characteristics of InGaAs APD spectral response. As the temperature rises, the InGaAs band gap energy becomes smaller, making the cutoff wavelength longer.
InGaAs APDs have an anti-reflection film formed on the light incident surfaces in order to prevent the quantum efficiency from deteriorating by reflection on the APD.

Terminal capacitance vs. reverse voltage characteristics

The graph curve of terminal capacitance vs. reverse voltage characteristics for InGaAs APDs differs from that of InGaAs PIN photodiodes [Figure 2-7]. This is because their PN junction positions are different.

[Figure 2-7] Terminal capacitance vs. reverse voltage (G14858-0020AA)

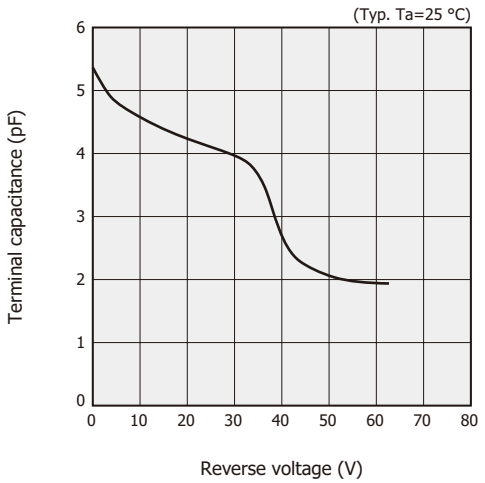

KAPDB0418EA

Noise characteristics

In InGaAs APDs, the gain for each carrier has statistical fluctuations. Multiplication noise known as excess noise is therefore added during the multiplication process. The InGaAs APD shot noise (In) becomes larger than the InGaAs PIN photodiode shot noise, and is expressed by equation (2-3).

$$In^2 = 2q\,(I_L + I_{DG})\,B\,M^2\,F + 2q\,I_{DS}\,B \quad \cdots\cdots\cdots \quad (2\text{-}3)$$

q : electron charge
I_L : photocurrent at M=1
I_{DG} : dark current component multiplied
I_{DS} : dark current component not multiplied
B : bandwidth
M : gain
F : excess noise factor

The number of electron-hole pairs generated during the time that a carrier moves a unit distance in the semiconductor is referred to as the ionization rate. The ionization rate of electrons is defined as "α" [cm^{-1}] and that of holes as "β" [cm^{-1}]. These ionization rates are important parameters that determine the multiplication mechanism. The ratio of β to α is called the ionization rate ratio (k), which is a parameter that indicates the InGaAs APD noise.

$$k = \frac{\beta}{\alpha} \quad \cdots\cdots\cdots\cdots \quad (2\text{-}4)$$

The ionization rate ratio is a physical constant inherent to individual semiconductor materials. The ionization rate ratio (k) for InP is greater than 1 since the hole ionization rate is larger than the electron ionization rate. Therefore, in InGaAs APDs, the holes of the electron-hole pairs generated by light absorption in the InGaAs layer will drift toward the InP avalanche layer due to the reverse voltage.
The excess noise factor (F) is expressed using the ionization rate ratio (k) as in equation (2-5).

$$F = M\,k + \left(2 - \frac{1}{M}\right)(1 - k) \quad \cdots\cdots\cdots\cdots \quad (2\text{-}5)$$

The excess noise factor can also be approximated as $F=M^x$ (where x is the excess noise index). Figure 2-8 shows an example of the relationship between the InGaAs APD excess noise factor and the gain. In this figure, the excess noise index is approximately 0.7.

[Figure 2-8] Excess noise factor vs. gain (G14858-0020AA)

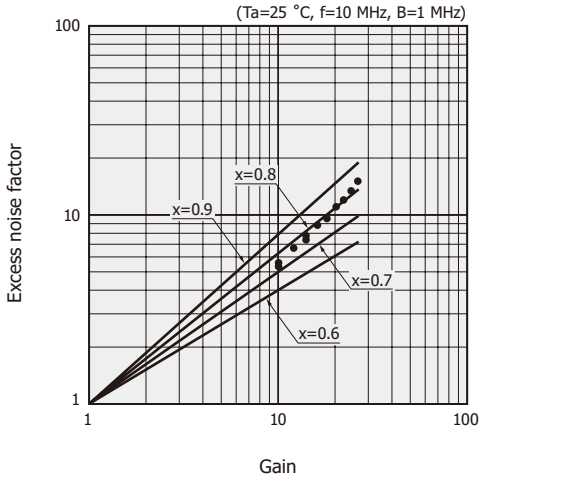

KIRDB0682EA

As already explained, InGaAs APDs generate noise accompanying the multiplication process, so excess noise increases as the gain becomes higher. The output signal also increases as the gain becomes higher, so the S/N is maximized at a certain gain. The S/N for an InGaAs APD can be expressed by equation (2-6).

$$S/N = \frac{I_L^2 M^2}{2q (I_L + I_{DG}) B M^2 F + 2q I_{DS} B + \frac{4k T B}{R_L}} \quad \cdots\cdots (2\text{-}6)$$

$2q (I_L + I_{DG}) B M^2 F$: excess noise
$2q I_{DS} B$: shot noise
k : Boltzmann's constant
T : absolute temperature
R_L: load resistance

The optimal gain (Mopt) can be found from conditions that maximize the value of equation (2-6), and given by equation (2-7) if I_{DS} is ignored.

$$Mopt = \left[\frac{4k T}{q (I_L + I_{DG}) \cdot x \cdot R_L}\right]^{\frac{1}{2+x}} \quad \cdots\cdots (2\text{-}7)$$

[Figure 2-9] Signal power, noise power, and S/N vs. gain

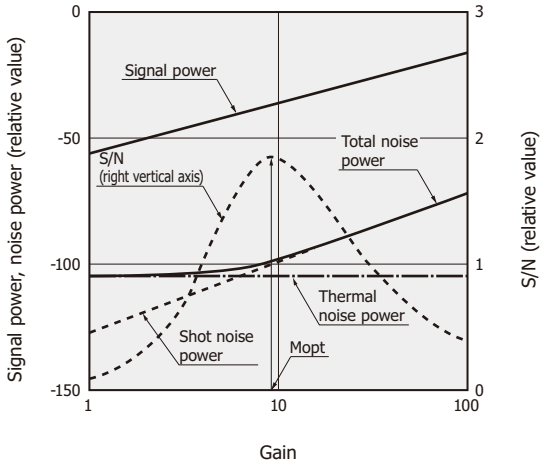

KIRDB0400EA

Response speed

Major factors that determine the response speed of an APD are the CR time constant, drift time (time required for the carrier to traverse the depletion layer), and the multiplication time. The cutoff frequency determined by the CR time constant is given by equation (2-8).

$$fc(CR) = \frac{1}{2\pi Ct R_L} \quad \cdots\cdots (2\text{-}8)$$

Ct: terminal capacitance
R_L: load resistance

To increase the cutoff frequency determined by the CR time constant, the terminal capacitance should be reduced. This means that a smaller photosensitive area with a thicker depletion layer is advantageous for raising the cutoff frequency. The relationship between cutoff frequency (fc) and the rise time (tr) is expressed by equation (2-9).

$$tr = \frac{0.35}{fc(CR)} \quad \cdots\cdots (2\text{-}9)$$

The drift time cannot be ignored if the depletion layer is made thick. The drift time trd and cutoff frequency fc(trd) determined by the drift time are expressed by equations (2-10) and (2-11), respectively.

$$trd = \frac{W}{vds} \quad \cdots\cdots (2\text{-}10)$$

$$fc(trd) = \frac{0.44}{trd} \quad \cdots\cdots (2\text{-}11)$$

W : thickness of depletion layer
vds: drift speed

The hole drift speed in InGaAs becomes saturated at an electric field strength of approx. 10^4 V/cm, and the drift speed at that point is approx. 5×10^6 cm/s. A thinner depletion layer is advantageous in improving the cutoff frequency fc(trd) determined by the drift time, so the cutoff frequency fc(trd) determined by the drift time has a trade-off relation with the cutoff frequency fc(CR) determined by the CR time constant.
The carriers passing through the avalanche layer repeatedly collide with the crystal lattice, so a longer time is required to move a unit distance than the time required to move in areas outside the avalanche layer. The time (multiplication time) required for the carriers to pass through the avalanche layer becomes longer as the gain increases.
In general, at a gain of 5 to 10, the CR time constant and drift time are the predominant factors in determining the response speed, and at a gain higher than 10, the multiplication time will be the predominant factor.
One cause that degrades the response speed in a low

gain region is a time delay due to the diffusion current of carriers from outside the depletion layer. This time delay is sometimes as large as a few microseconds and appears more prominently in cases where the depletion layer has not extended enough versus the penetration depth of incident light into the InGaAs.

To achieve high-speed response, it is necessary to apply a reverse voltage higher than a certain level, so that the InGaAs light absorption layer becomes fully depleted. If the InGaAs light absorption layer is not fully depleted, the carriers generated by light absorbed outside the depletion layer might cause "trailing" that degrades the response characteristics.

When the incident light level is high and the resulting photocurrent is large, the attraction force of electrons and holes in the depletion layer serves to cancel out the electric field, so the carrier drift speed in the InGaAs light absorption layer becomes slower and time response is impaired. This phenomenon is called the space charge effect and tends to occur especially when the optical signal is interrupted.

» Sensitivity uniformity of photosensitive area

Since a large reverse voltage is applied to InGaAs APDs to apply a high electric field across the PN junction, this electric field might concentrate locally especially at or near the junction and tend to cause breakdowns. To prevent this, Hamamatsu InGaAs APDs use a structure having a guard ring formed around the PN junction. This ensures uniform sensitivity in the photosensitive area since the electric field is applied uniformly over the entire photosensitive area.

[Figure 2-10] Sensitivity distribution in photosensitive area (G14858-0020AA)

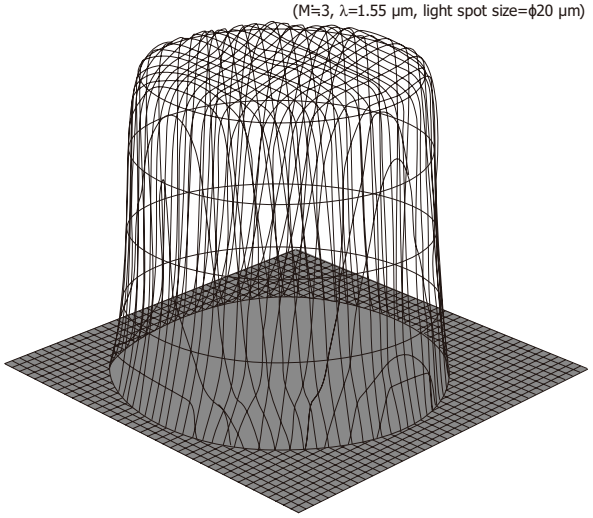

KIRDB0683EA

2 - 3 How to use

InGaAs APDs can be handled nearly the same as InGaAs PIN photodiodes and Si APDs. However, the following precautions should be taken.

① The absolute maximum rating of the reverse current for InGaAs APDs is 2 mA. So there is a need to add a protective resistor and then install a current limiting circuit to the bias circuit.

② A low-noise readout circuit may damage the first stage in response to excess voltage. To prevent this, a protective circuit should be connected to divert any excess input voltage to the power supply voltage line.

③ APD gain changes with temperature. To use an APD over a wide temperature range, the reverse voltage must be controlled to match the temperature changes or the APD temperature must be maintained at a constant level.

④ When detecting low-level light signals, the lower detection limit is determined by the shot noise. If background light enters the APD, then the S/N might deteriorate due to shot noise from background light. In this case, effects from the background light must be minimized by using optical filters, improving laser modulation, and/or restricting the angle of view. Because of their structure, the excess noise index for InGaAs APDs is especially large compared to Si APD, so effects from shot noise including excess noise must be taken into account.

A connection example is shown in Figure 2-11. We welcome requests for customization of InGaAs APD modules.

[Figure 2-11] Connection example

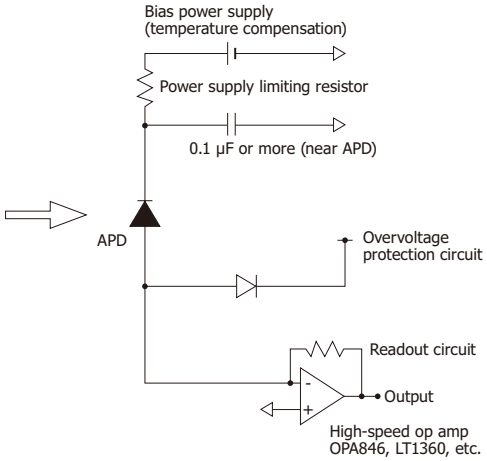

KIRDC0079EB

3. InAs/InAsSb/InSb photovoltaic detectors

As with InGaAs PIN photodiodes, InAs/InAsSb/InSb photovoltaic detectors are infrared detectors having a PN junction. InAs photovoltaic detectors are sensitive around 3 µm, the same as PbS photoconductive detectors, while InSb photovoltaic detectors are sensitive to the 5 µm band, the same as PbSe photoconductive detectors. InAsSb photovoltaic detectors deliver high sensitivity in the 5 µm, 8 µm, or 10 µm band.

3 - 1 Characteristics

» Spectral response

Controlling the composition of $InAs_xSb_{1-x}$, which is a III-V family compound semiconductor material, enables the fabrication of detectors whose cutoff wavelength at room temperature ranges from 3.3 µm (InAs) to 12 µm ($InAs_{0.38}Sb_{0.62}$).

[Figure 3-1] Band gap energy and peak sensitivity wavelength vs. composition ratio x of $InAs_xSb_{1-x}$

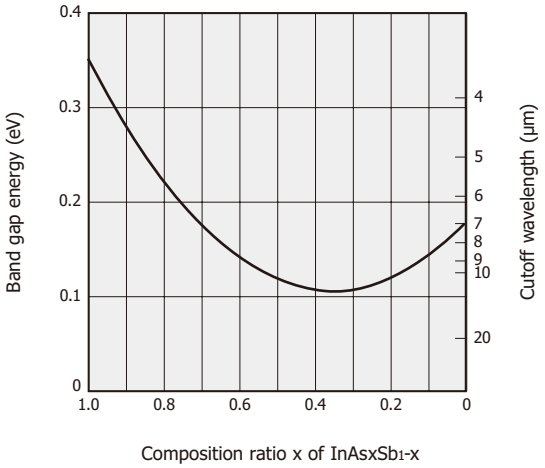

KIRDB0406EB

InAs photovoltaic detectors include a non-cooled type, TE-cooled type (Tchip=-10 °C, -30 °C), and liquid nitrogen cooled type (Tchip=-196 °C) which are used for different applications. InAsSb photovoltaic detectors are available in non-cooled type and TE-cooled type (Tchip=-30 °C), and the non-cooled type includes a type with a band-pass filter and a two-element type that can detect two wavelengths. InSb photovoltaic detectors are only available as liquid nitrogen cooled types. Figure 3-2 shows spectral responses of InAs/InAsSb/InSb photovoltaic detectors. Cooling these detectors shifts their cutoff wavelengths to the shorter wavelength side.

[Figure 3-2] Spectral response

(a) InAs photovoltaic detectors

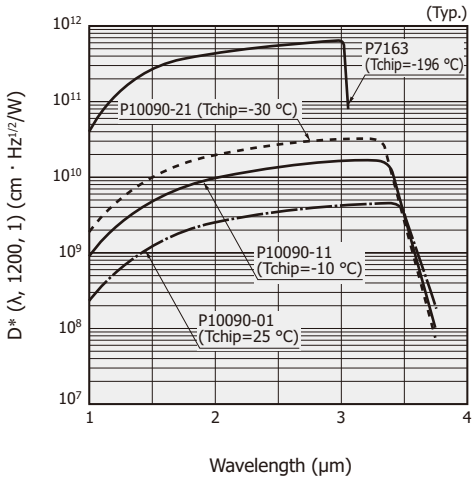

KIRDB0356EF

(b) InAsSb photovoltaic detectors (cutoff wavelength: 5 µm band)

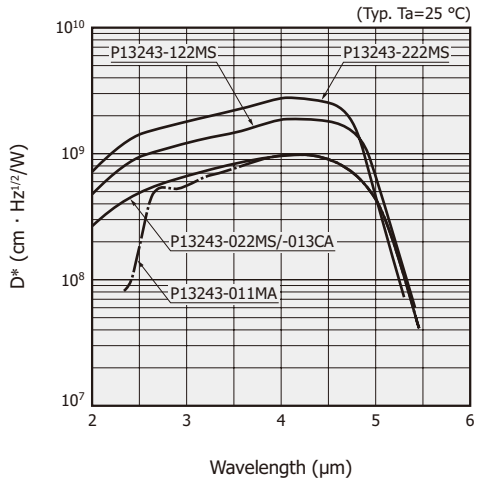

KIRDB0658ED

(c) InAsSb photovoltaic detectors with band-pass filter

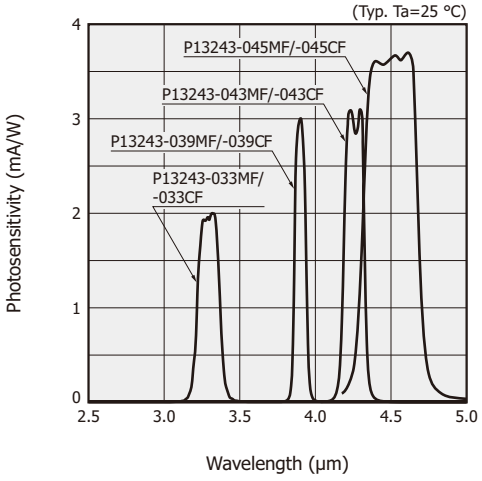

KIRDB0676EB

(d) InAsSb photovoltaic detectors
(cutoff wavelength: 10 µm band)

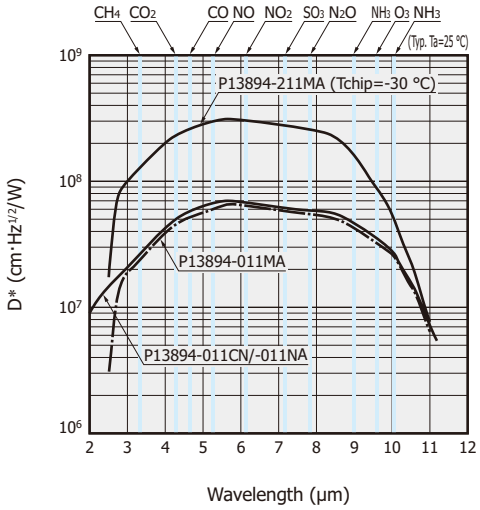

KIRDB0632EB

(e) InSb photovoltaic detectors

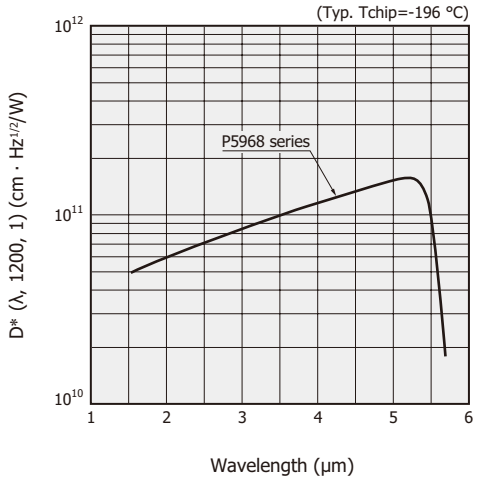

KIRDB0063EC

Noise characteristics

InAs/InAsSb/InSb photovoltaic detector noise (i) results from Johnson noise (ij) and shot noise (i_{SD}) due to dark current (including photocurrent generated by background light). Each type of noise is expressed by the following equations:

$$i = \sqrt{ij^2 + i_{SD}^2} \cdots\cdots (3\text{-}1)$$

$$ij = \sqrt{4k\,T\,B/Rsh} \cdots\cdots (3\text{-}2)$$

$$i_{SD} = \sqrt{2q\,I_D\,B} \cdots\cdots (3\text{-}3)$$

k : Boltzmann's constant
T : absolute temperature of element
B : noise bandwidth
Rsh: shunt resistance
q : electron charge
I_D : dark current

When considering the spectral response range of InSb photovoltaic detectors, background light fluctuations (background radiation noise) from the surrounding areas cannot be ignored. The D* of photovoltaic detectors is given by equation (3-4) assuming that the background radiation noise is the only noise source.

$$D^* = \frac{\lambda\sqrt{\eta}}{h\,c\sqrt{2Q}} \ [cm \cdot Hz^{1/2}/W] \cdots\cdots (3\text{-}4)$$

λ : wavelength
η : quantum efficiency
h : Planck's constant
c : speed of light
Q: background photon flux [photons/cm^2·s]

To reduce background radiation noise, the detector's field of view (FOV) must be limited by using a cold shield or unwanted wavelengths must be eliminated by using a cooled band-pass filter. Figure 3-4 shows how the D* relates to the field of view.

[Figure 3-3] Field of view (FOV)

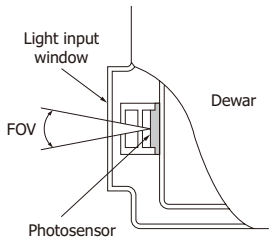

KIRDC0033EB

[Figure 3-4] D* vs. field of view (P5968-060, typical example)

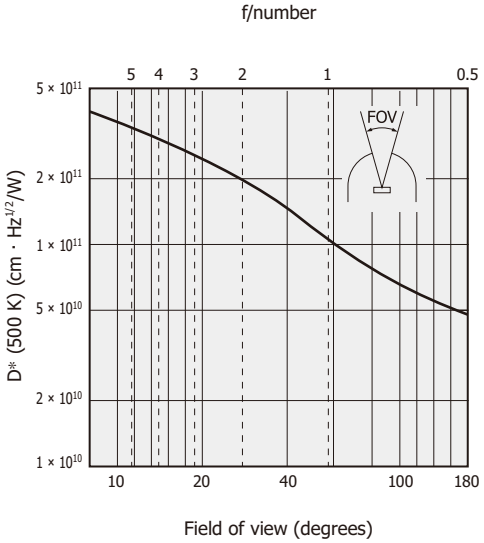

KIRDB0138EC

3 - 2 How to use

Operating circuit

Figure 3-5 shows connection examples for InAs/InAsSb/InSb photovoltaic detectors. The photocurrent is extracted as a voltage using a load resistor or op amp. When connecting an op amp to an InAs/InAsSb photovoltaic detector with low shunt resistance, we recommend the use of an op amp with low voltage noise.

[Figure 3-5] Connection examples

(a) When load resistor is connected

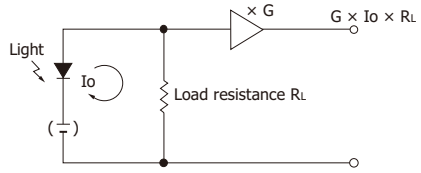

(b) When op amp is connected

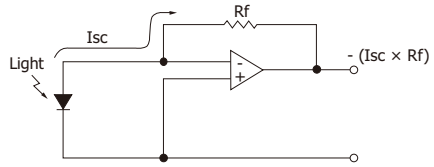

KPDC0006EC

Light incidence

The P12691-201G has a lens built in the product, so it uses collimated light for light incidence. Focusing light in front of the detector may reduce the output.
When using the P13243 series or P13894 series, it is necessary to irradiate the entire photosensitive area uniformly. If you irradiate only a part of the photosensitive area, the output signal may become smaller and linearity may deteriorate [Figure 3-6].

[Figure 3-6] Linearity (P13243 series, typical example)

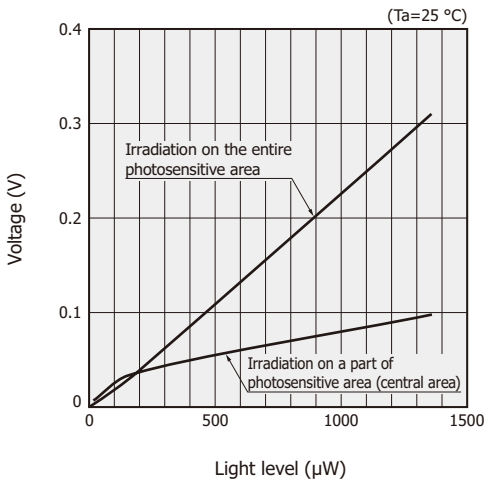

KIRDB0691EA

Shunt resistance measurement

Measuring the shunt resistance of InAs/InAsSb/InSb photovoltaic detectors with a multimeter or the like might destroy the detectors. During measurement, the reverse voltage applied to the detector must be the absolute maximum rating value or less. The cooled type is easily destroyed if the shunt resistance is measured at room temperature, so be sure to measure it in a cooled state.

4. Type Ⅱ superlattice infrared detector

Type Ⅱ superlattice infrared detector is a photovoltaic detector with sensitivity expanded to the 14 µm band using Hamamatsu unique crystal growth technology and process technology. This product is an environmentally friendly infrared detector and does not use mercury or cadmium, which are substances restricted by the RoHS Directive. It is a replacement for conventional products that contain these substances.

4 - 1 Structure

By stacking thin films of InAs and GaSb alternately, energy bands (minibands) which are not found in bulk crystals are formed. The position of the miniband can be controlled by changing its thickness and composition.

[Figure 4-1] Cross-sectional structure and energy levels

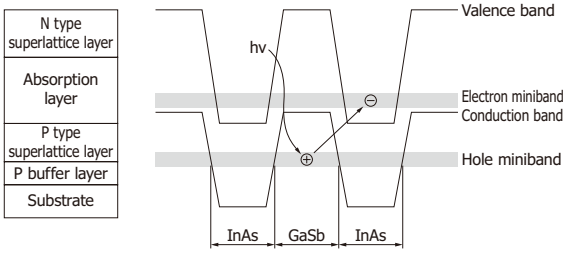

KIRDC0132EA

4 - 2 Characteristics

Spectral response

Type Ⅱ superlattice infrared detector is liquid nitrogen cooled type. Figure 4-2 shows spectral response.

[Figure 4-2] Spectral response

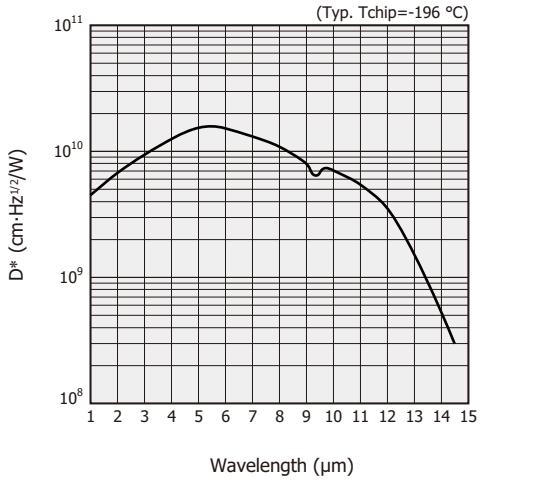

KIRDB0673EB

Linearity

The linearity of type II superlattice infrared detectors is about two orders of magnitude better than a conventional MCT photoconductive detector.

[Figure 4-3] Linearity

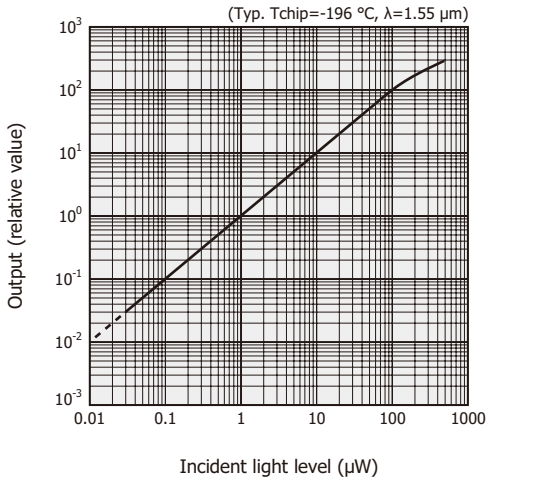

KIRDB0677ED

4 - 3 How to use

Operating circuit

Using an op amp, the photocurrent is converted into voltage and then the converted voltage is output. For details, see "1. InGaAs PIN photodiodes | 1-2 How to use (P.8)".

Background radiation

In infrared measurement, background radiation that is not the signal light affects the measurement. Use a cold shield to set the proper FOV, so as to avoid detecting background radiation.

5. Two-color detectors

Two-color detectors are infrared detectors that use two or more vertically stacked detectors to extend the spectral response range. We provide products with a Si mounted as the light incident surface over an InGaAs along the same optical axis as well as products with a standard type InGaAs mounted over a long wavelength type InGaAs. Other combinations such as Si and InAs or InAsSb are available. The upper detector not only detects infrared light but also serves as a short-wavelength cutoff filter for the lower detector.

[Figure 5-1] Dimensional outlines (Si + InGaAs, unit: mm)

(a) Metal package

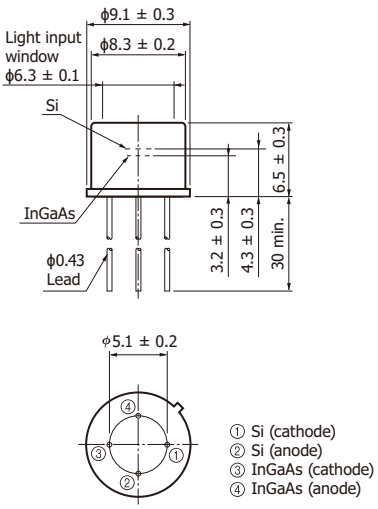

KIRDA0147EB

(b) Ceramic package

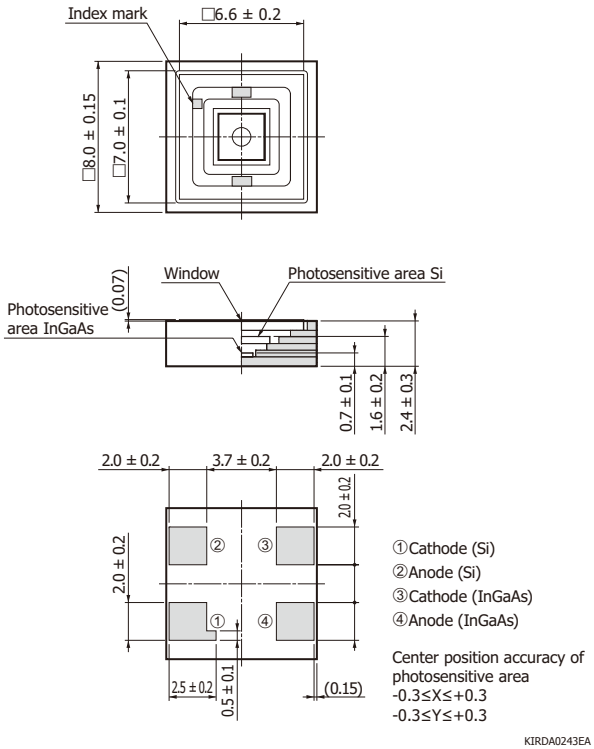

KIRDA0243EA

[Figure 5-2] Spectral response

(a) Si + InGaAs

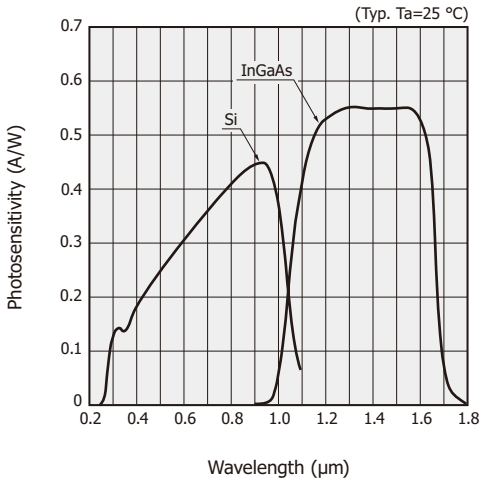

KIRDB0405EB

(b) Standard type InGaAs + long wavelength type InGaAs

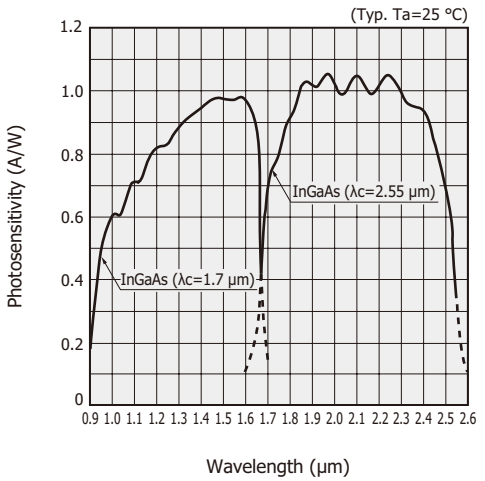

KIRDB0479EB

6. New approaches

6 - 1 Ultra high-speed InGaAs PIN photodiodes

As ultra high-speed response photosensors, the product demand for higher-speed photodiodes is on the rise in addition to 25 Gbps and 50 Gbps photodiodes. In this case, it is essential to keep the cost of the system itself from rising, so low power consumption and ease of assembling are required. To ensure the S/N, reduction in sensitivity from previous products is not acceptable. The photodiodes must maintain the present photosensitivity as much as possible and operate at high speed under a low reverse voltage. At the same time, the manufacturing process must integrate optical techniques to guide as much light as possible into a small photosensitive area. We have produced an ultra high-speed InGaAs PIN photodiode that operates from a low reverse voltage and verified its operation on transmission bands up to 64 Gbps at V_R=2 V in combination with an optimum preamp. We are currently working to achieve even higher speeds.

[Figure 6-1] Frequency characteristics

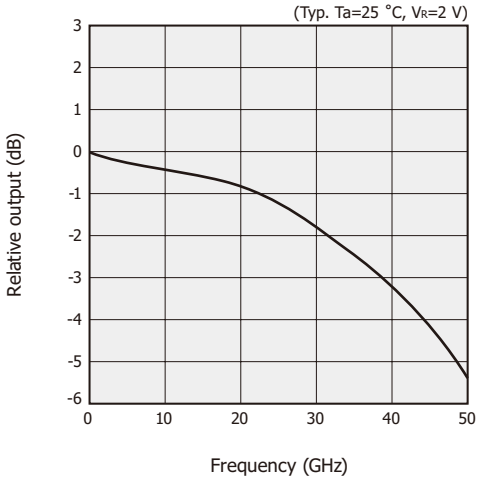

KIRDB0685EA

7. Options

Hamamatsu offers amplifiers, temperature controllers, heatsinks, chopper, cables, and the like as compound semiconductor photosensor options. Temperature controllers and heatsinks are for TE-cooled types. Temperature controllers are used to maintain the element temperature at a constant level, and heatsinks are used to radiate heat efficiently from the TE coolers. Choppers can be used to modulate only the detected light to separate it from the background light when performing infrared detection. This helps to reduce the effect of background light. Furthermore, we also provide infrared detector modules that integrate an infrared detector and preamp.

[Figure 7-1] Connection example of options for compound semiconductor photosensors

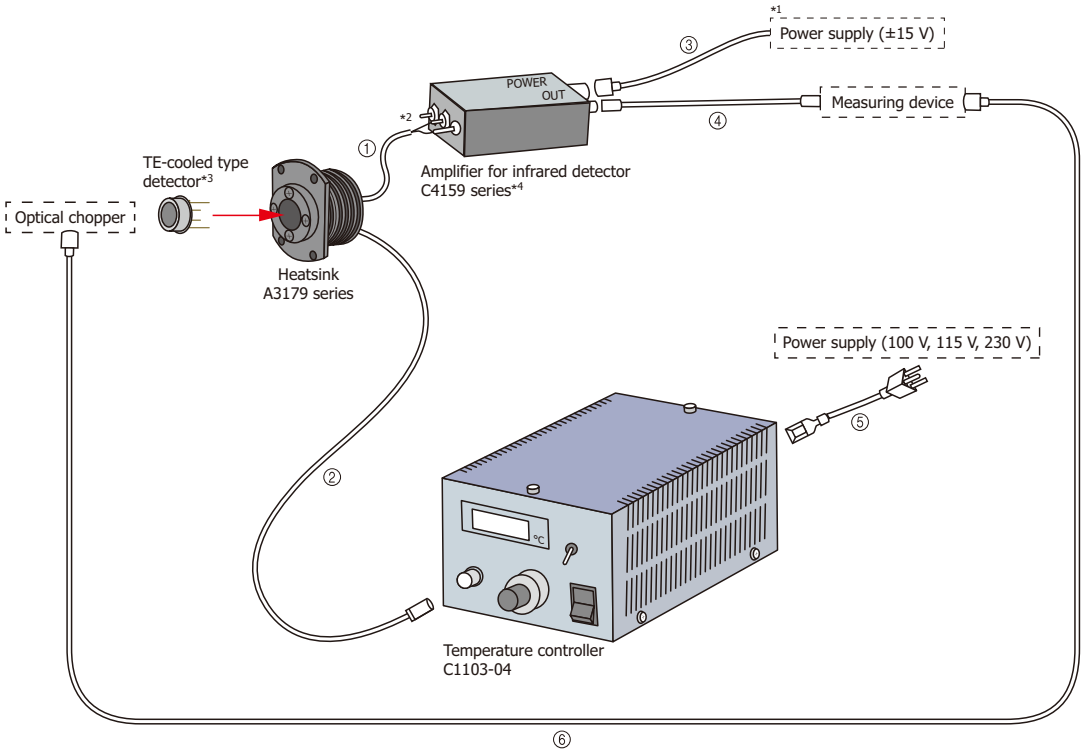

KACC0321EE

Cable no.	Cable	Approx. length	Remarks
①	Coaxial cable (for signal)	2 m	Supplied with heatsink A3179 series. Make the cable as short as possible. (About 10 cm is desirable.)
②	4-conductor cable (with a connector) A4372-05	3 m	Supplied with temperature controller C1103 series. It is also sold separately.
③	Power supply cable (with a 4-conductor connector) A4372-02	2 m	Supplied with C4159/C5185 series and C3757-02 amplifiers for infrared detectors and infrared detector modules with preamp (room temperature type). It is also sold separately.
④	BNC connector cable E2573	1 m	Sold separately
⑤	Power supply cable (for temperature controller)	1.9 m	Supplied with temperature controller C1103 series
⑥	Cable	-	Prepared by user

*1: Attach the unterminated wire to a 3-4 pin connector or banana plug, then connect it to the power supply.
*2: Soldering is required.
*3: No dedicated socket is available. Soldering is required.
*4: Refer to amplifiers for infrared detectors.

8. Applications

8 - 1 Optical power meters

Optical power meters measure light level and are used in a wide range of applications including optical fiber communications and laser beam detection. Optical fiber communications are grouped into two categories: short/middle distance and long distance communications. In long distance communications, infrared light in the 1.3 and 1.55 µm wavelength bands, which has less optical loss during transmission through optical fibers, is used. In these wavelength bands, InGaAs PIN photodiodes are used to measure transmission loss in optical fibers, check whether relays are in satisfactory condition, and measure laser power. Major characteristics required of optical power meters are linearity and uniformity. In some cases, cooled type detectors are used to reduce the noise levels so that even low-power light can be detected.

[Figure 8-1] Optical power meter

KIRDC0100EA

8 - 2 LD monitors

The output level and emission wavelength of LD (laser diodes) vary with the LD temperature. So APC (automatic power control) is used to stabilize the LD. APC includes two methods. One method monitors the integrated amount of light pulses from the LD, and the other monitors the peak values of light pulses. Along with the steady increase in LD output power, linearity at higher light levels has become important for the detectors used in these monitors. High-speed response is also required to monitor the peak values of light pulses.

InGaAs PIN photodiodes used for LD monitors are mounted either in the same package as the LD or outside the LD package. Also, InAs and InSb photovoltaic detectors are used to monitor lasers at even longer wavelengths.

[Figure 8-2] LD monitor

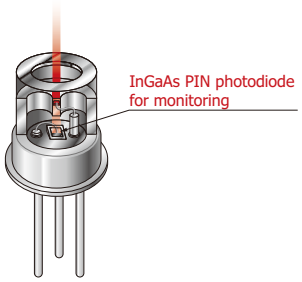

KIRDC0096EB

8 - 3 OTDR

The OTDR (optical time domain reflectometer) is a measuring instrument that can detect the loss point and the connection state between fibers, as well as attenuation in the optical fiber. The OTDR must detect very weak signals, so an InGaAs APD is used as the sensor.

[Figure 8-3] OTDR measurement

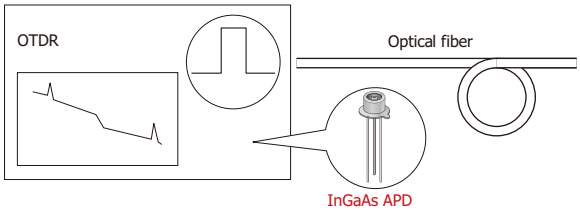

KIRDC0129EA

8 - 4 Optical communication from 100 Gbps to 400 Gbps

As the amount of data traffic in optical communication networks increases, the transceivers used are also increasing in speed from 100 Gbps to 400 Gbps. An ultra high-speed InGaAs PIN photodiode is used for the optical communication receiver.

[Figure 8-4] Optical communication network

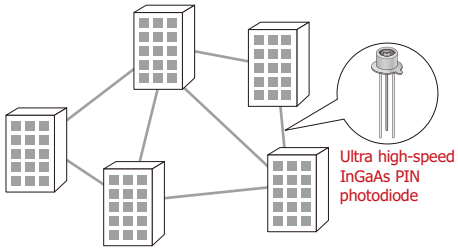

KIRDC0130EA

8 - 5 Radiation thermometers

Any object higher than absolute zero degrees radiates infrared light matching its own temperature. The quantity of infrared light actually emitted from an object is not directly determined just by the object temperature but must be corrected according to the object's emissivity (e). Figure 8-5 shows the radiant energy from a black body. The black body is e=1. Figure 8-6 shows the emissivity of various objects. The emissivity varies depending on temperature and wavelength.
The noise equivalent temperature difference (NEΔT) is used as one measure for indicating the temperature resolution. NEΔT is defined in equation (8-1).

$$NE\Delta T = \frac{L_N}{\left.\frac{dL}{dT}\right|_{T=T_1}} \quad \cdots\cdots\cdots (8\text{-}1)$$

L_N: noise equivalent luminance
T_1: temperature of object

Noise equivalent luminance (L_N) relates to the detector NEP as shown in equation (8-2).

$$NEP = To\ L_N\ \Omega\ Ao\ /\ \gamma \quad \cdots\cdots\cdots (8\text{-}2)$$

To : optical system loss
Ω : solid angle from optical system toward measurement area
Ao: aperture area of optical system
γ : circuit system loss

$\left.\frac{dL}{dT}\right|_{T=T_1}$ in equation (8-1) represents the temperature coefficient of radiant luminance (L) from an object at temperature T_1. The radiant luminance can be obtained by integrating the spectral radiant exitance over the wavelength range (λ_1 to λ_2) being observed.

$$L = \int_{\lambda_1}^{\lambda_2} \frac{1}{\pi} M\lambda\, d\lambda \quad \cdots\cdots\cdots (8\text{-}3)$$

$M\lambda$: spectral radiant exitance

Radiation thermometers offer the following features compared to other temperature measurement methods.

· Non-contact measurement avoids direct contact with object.
· High-speed response
· Easy to make pattern measurements

Infrared detectors for radiation thermometers should be selected according to the temperature and material of the object to be measured. For example, peak emissivity wavelength occurs at around 5 µm in glass materials and around 3.4 µm or 8 µm in plastic films, so a detector sensitive to these wavelength regions must be selected.
Infrared detectors combined with an infrared fiber now make it possible to measure the temperature of objects in hazardous locations such as complex internal structures, and objects in a hot, vacuum, or in high-pressure gases.

[Figure 8-5] Black body radiation law (Planck's law)

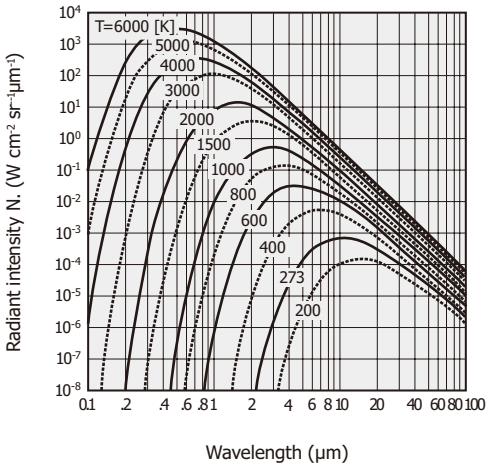

KIRDB0014EB

[Figure 8-6] Emissivity of various objects

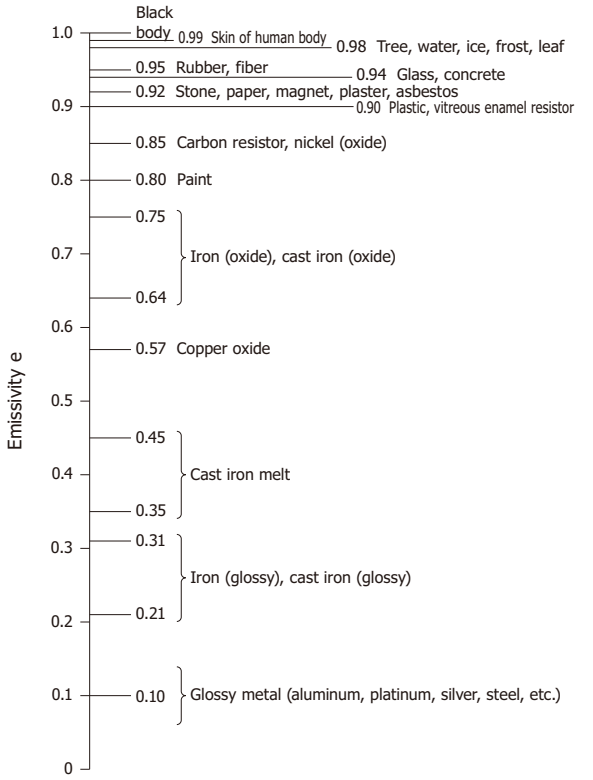

KIRDC0036EA

[Figure 8-7] Transmittance and reflectance of glass vs. wavelength

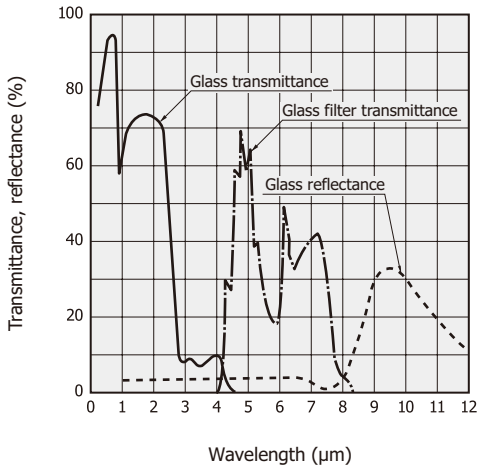

KIRDB0146EA

8 - 6 Distance measurement (e.g., LiDAR)

Distance to a target object can be measured at high speeds and high accuracy by directing a laser beam at the target object and detecting the reflected low-level light. The InGaAs APD achieves high S/N when it is applied with a reverse voltage and is suitable for low-level-light measurement. It is commonly used as a distance measurement sensor because it can detect light at an eye-safe wavelength of 1.55 µm.

[Figure 8-8] Distance measurement

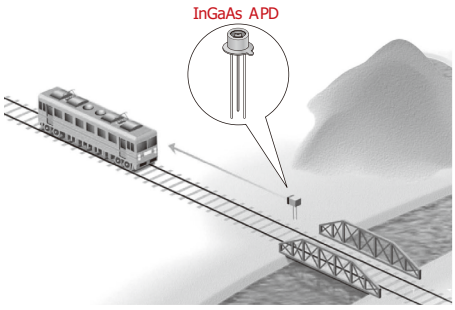

KIRDC0098EA

8 - 7 Flame eyes (flame monitors)

Flame eyes detect light emitted from flames to monitor the flame burning state. Radiant wavelengths from flames cover a broad spectrum from the ultraviolet to infrared region as shown in Figure 8-9. Flame detection methods include detecting a wide spectrum of light from ultraviolet to infrared using a two-color detector, and detecting near infrared region or light with 4.26 µm wavelength using an InAsSb photovoltaic detector.

[Figure 8-9] Radiant spectrum from flame

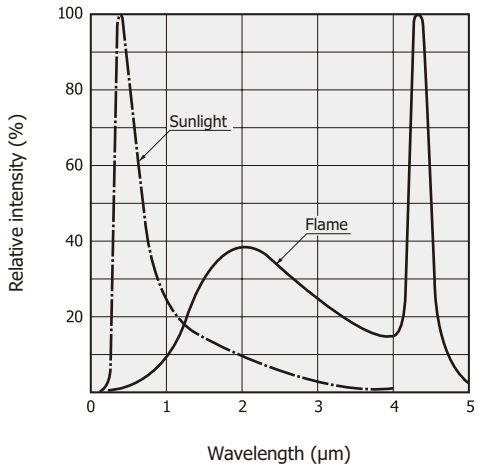

KIRDB0147EA

8 - 8 Moisture meters

Moisture meters measure the moisture of objects such as food by illuminating the object with reference light and with near infrared light at water absorption wavelengths (1.1 µm, 1.4 µm, 1.9 µm, 2.7 µm). The two types of light reflected from or transmitted through the object are detected, and their ratio is calculated to measure the moisture level of the object. Photosensors suited for moisture measurement include InGaAs PIN photodiodes and InAs photovoltaic detectors.

8 - 9 Gas analyzers

Gas analyzers measure gas concentrations by making use of the fact that gases absorb specific wavelengths of light in the infrared region. Gas analyzers basically utilize two methods: a dispersive method and a non-dispersive method. The dispersive method disperses infrared light from a light source into a spectrum and measures the absorption amount at each wavelength to determine the constituents and quantities of the sample. The non-dispersive method measures the absorption amounts only at particular wavelengths. The non-dispersive method is currently the method mainly used for gas analysis. Non-dispersive method gas analyzers are used for measuring automobile exhaust gases (CO, CH, CO_2) and exhaled respiratory gas components (CO_2), as well as for regulating fuel exhaust gases (COx, SOx, NOx) and detecting fuel leaks (CH_4, C_2H_6). Further applications include CO_2 (4.26 µm) measurements in carbonated beverages (soft drinks, beer, etc.) and sugar content (3.9 µm) measurement. Figure 8-10 shows absorption spectra of various gases.

Hamamatsu provides InGaAs, InAs, InAsSb, InSb, and the like. as sensors to measure the various light wavelengths. Quantum cascade lasers (QCL; middle

infrared semiconductor lasers) are also available for use in gas analyzers. There is a lineup of products with specific oscillation wavelength in the middle infrared region (4 to 10 µm).

[Figure 8-10] Gas absorption spectra

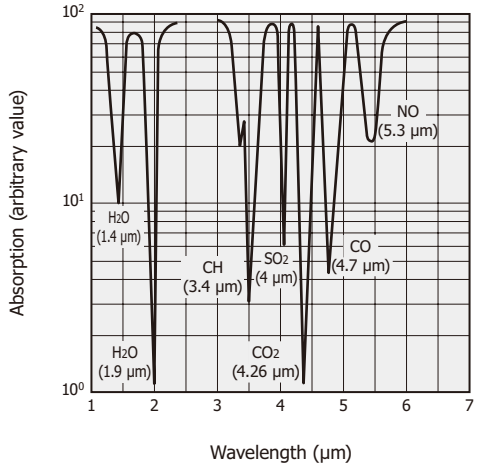

KIRDB0148EB

8 - 10 Infrared imaging devices

Infrared imaging devices are finding a wide range of applications from industry to medical imaging, academic research, and many other fields [Table 8-1]. The principle of infrared imaging is grouped into two techniques. One technique uses a one-dimensional array as a detector and captures an image by scanning the optical system from the Z axis. The other technique uses a two-dimensional array and so does not require scanning the optical system.

Even higher quality images can be acquired with InAsSb photovoltaic detectors, QWIP (quantum well infrared photodetector), thermal detectors utilizing MEMS technology, and two-dimensional arrays fabricated by heterojunction to CMOS circuitry.

8 - 11 Remote sensing

Light emitted or reflected from objects contains different information depending on the wavelength as shown in Figure 8-11. Measuring this light at each wavelength allows obtaining various information specific to the object. Among the various measurements, infrared remote sensing can acquire information such as the surface temperature of solids or liquids, or the type and temperature of gases. Remote sensing from space satellites and airplanes is recently becoming increasingly used to obtain global and macroscopic information such as the temperature of the earth's surface or sea surface and the gas concentration in the atmosphere. Information obtained in this way is utilized for environmental measurement, weather observation, and resource surveys.

[Figure 8-11] Optical system for resource survey

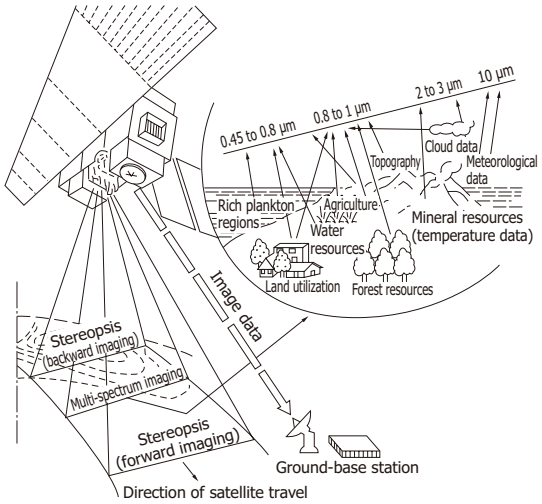

KIRDC0039EB

[Table 8-1] Infrared imaging device application fields

Application field	Applications
Industry	Process control for steel and paper, non-destructive inspection of welds or soldering, non-destructive inspection of buildings and structures, evaluating wafers and IC chips, inspecting and maintaining power transmission lines and electric generators, heat monitoring of shafts and metal rolling, marine resource surveys, forest distribution monitoring
Pollution monitor	Monitoring of seawater pollution and hot wastewater
Academic research	Geological surveys, water resource surveys, ocean current research, volcano research, meteorological investigations, space and astronomical surveys
Medical imaging	Infrared imaging diagnosis (diagnosis of breast cancer and the like)
Security and surveillance	Monitoring of boiler temperatures, fire detection, gas leak detection
Automobile, airplane	Night vision device for visual enhancement, engine evaluations

8 - 12 FTIR

The FTIR (Fourier transform infrared spectrometer) is an instrument that acquires a light spectrum by Fourier-transforming interference signals obtained with a double-beam interferometer. It has the following features:

· High power of light due to non-dispersive method (simultaneous measurement of multiple spectral elements yields high S/N)
· High wavelength accuracy

The following specifications are required for infrared detectors that form the core of the FTIR.

· Wide spectral response range
· High sensitivity
· Photosensitive area size matching the optical system
· Wide frequency bandwidth
· Excellent linearity versus incident light level

Thermal type detectors are generally used over a wide spectral range from 2.5 µm to 25 µm. Quantum type detectors such as InAs, InAsSb, and InSb are used in high-sensitivity and high-speed measurements.

8 - 13 Black plastic sorting

Recycling plastics is becoming increasingly important as an effort to reduce environmental impact. There are many kinds of plastics, and sorting them out is essential. Many plastics have characteristic peaks in the near infrared region, so they are sorted using near infrared light. However, in black plastic, mid infrared light is used for sorting because near infrared light is absorbed by the pigment carbon black, etc. InAsSb photovoltaic detectors are suitable as photodetectors for the mid infrared region.

[Figure 8-12] Absorption spectrum of black plastics

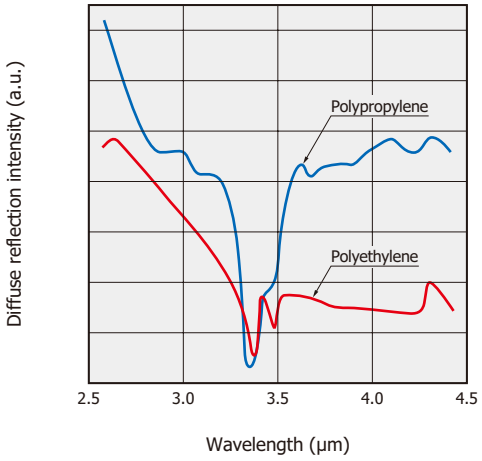

Data provided by Professor Hirofumi Kawazumi
(Faculty of Humanity-oriented Science and Engineering, Kindai University)

KIRDB0701EA

HAMAMATSU

www.hamamatsu.com

HAMAMATSU PHOTONICS K.K., Solid State Division
1126-1 Ichino-cho, Higashi-ku, Hamamatsu City, 435-8558 Japan, Telephone: (81)53-434-3311, Fax: (81)53-434-5184
U.S.A.: HAMAMATSU CORPORATION: 360 Foothill Road, Bridgewater, NJ 08807, U.S.A., Telephone: (1)908-231-0960, Fax: (1)908-231-1218 E-mail: usa@hamamatsu.com
Germany: HAMAMATSU PHOTONICS DEUTSCHLAND GMBH.: Arzbergerstr. 10, 82211 Herrsching am Ammersee, Germany, Telephone: (49)8152-375-0, Fax: (49)8152-265-8 E-mail: info@hamamatsu.de
France: HAMAMATSU PHOTONICS FRANCE S.A.R.L.: 19 Rue du Saule Trapu, Parc du Moulin de Massy, 91882 Massy Cedex, France, Telephone: (33)1 69 53 71 00, Fax: (33)1 69 53 71 10 E-mail: infos@hamamatsu.fr
United Kingdom: HAMAMATSU PHOTONICS UK LIMITED: 2 Howard Court,10 Tewin Road, Welwyn Garden City, Hertfordshire, AL7 1BW, UK, Telephone: (44)1707-294888, Fax: (44)1707-325777 E-mail: info@hamamatsu.co.uk
North Europe: HAMAMATSU PHOTONICS NORDEN AB: Torshamnsgatan 35 16440 Kista, Sweden, Telephone: (46)8-509 031 00, Fax: (46)8-509 031 01 E-mail: info@hamamatsu.se
Italy: HAMAMATSU PHOTONICS ITALIA S.R.L.: Strada della Moia, 1 int. 6, 20044 Arese (Milano), Italy, Telephone: (39)02-93 58 17 33, Fax: (39)02-93 58 17 41 E-mail: info@hamamatsu.it
China: HAMAMATSU PHOTONICS (CHINA) CO., LTD.: 1201 Tower B, Jiaming Center, 27 Dongsanhuan Beilu, Chaoyang District, 100020 Beijing, P.R. China, Telephone: (86)10-6586-6006, Fax: (86)10-6586-2866 E-mail: hpc@hamamatsu.com.cn
Taiwan: HAMAMATSU PHOTONICS TAIWAN CO., LTD.: 8F-3, No.158, Section 2, Gongdao 5th Road, East District, Hsinchu, 300, Taiwan R.O.C. Telephone: (886)3-659-0080, Fax: (886)3-659-0081 E-mail: info@hamamatsu.com.tw

Cat. No. KIRD9004E02 Aug. 2022 DN